JOURNAL OF GEOPHYSICAL RESEARCH, VOL. 113, D04201, doi:10.1029/2007JD008632, 2008

Increase of cloud droplet size with aerosol optical depth: An observation and modeling study

Tianle Yuan,[1] Zhanqing Li,[1,3] Renyi Zhang,[2] and Jiwen Fan[2,4]

Received 7 March 2007; revised 3 September 2007; accepted 23 October 2007; published 21 February 2008.

[1] Cloud droplet effective radius (DER) is generally negatively correlated with aerosol optical depth (AOD) as a proxy of cloud condensation nuclei. In this study, cases of positive correlation were found over certain portions of the world by analyzing the Moderate Resolution Imaging Spectroradiometer (MODIS) satellite products, together with a general finding that DER may increase or decrease with aerosol loading depending on environmental conditions. The slope of the correlation between DER and AOD is driven primarily by water vapor amount, which explains 70% of the variance in our study. Various potential artifacts that may cause the positive relation are investigated including the effects of aerosol swelling, partially cloudy, atmospheric dynamics, cloud three-dimensional (3-D) and surface influence effects. None seems to be the primary cause for the observed phenomenon, although a certain degree of influence exists for some of the factors. Analyses are conducted over seven regions around the world representing different types of aerosols and clouds. Only two regions show positive dependence of DER on AOD, near coasts of the Gulf of Mexico and South China Sea, which implies physical processes may at work. Using a 2-D Goddard Cumulus Ensemble model (GCE) with spectral-bin microphysics which incorporated a reformulation of the Köhler theory, two possible physical mechanisms are hypothesized. They are related to the effects of slightly soluble organics (SSO) particles and giant cloud condensation nuclei (CCN). Model simulations show a positive correlation between DER and AOD, due to a decrease in activated aerosols with an increasing SSO content. Addition of a few giant CCNs also increases the DER. Further investigations are needed to fully understand and clarify the observed phenomenon.

Citation: Yuan, T., Z. Li, R. Zhang, and J. Fan (2008), Increase of cloud droplet size with aerosol optical depth: An observation and modeling study, *J. Geophys. Res.*, *113*, D04201, doi:10.1029/2007JD008632.

1. Introduction

[2] Aerosol indirect effects (AIE) refer to any aerosol-induced alteration of cloud microphysics, cloud duration, precipitation, etc. While different types of AIE have been proposed [*Twomey*, 1977; *Albrecht*, 1989; *Kaufman and Fraser*, 1997], almost all are rooted to a fundamental change in cloud droplet size by aerosol. Twomey's hypothesis that cloud particle size is reduced by adding aerosols as cloud condensation nuclei (CCN) for a fixed liquid water amount is the foundation to many of the AIEs [*Twomey*, 1977], which has been supported with ample evidence from satellite [*Han et al.*, 1994; *Wetzel and Stowe*, 1999; *Nakajima et al.*, 2001; *Liu et al.*, 2003] and ground and in situ observations [*Leaitch et al.*, 1996; *Feingold et al.*, 2003; *Penner et al.*, 2004]. However, a large range of variation (by a factor of 3 or more) was found concerning the sensitivity of cloud microphysics to aerosol, as measured by the ratio of the change in cloud particle size to aerosol parameters. While some of the differences are related to the use of different analysis methods and/or observational data [*Rosenfeld and Feingold*, 2003], natural variation is observed [*Feingold et al.*, 2003; *Kim et al.*, 2003]. It is uncertain yet what drives the variation. Note that all previous studies showed a negative dependence of cloud particle size on aerosol loading. Some studies showed the opposite but did not elaborate on the finding [*Sekiguchi et al.*, 2003; *Strorelvmo et al.*, 2006].

[3] The impact of AIE on climate is generally measured in terms of aerosol radiative forcing, which is the difference in the radiation budget with and without the consideration of AIE. There have been estimations of the global aerosol indirect forcing (AIF) with large disparities [*IPCC*, 2001; *Anderson et al.*, 2003]. Models following forward calculations and inverse calculations have shown different magnitude of the global AIF. The forward calculations using observation-based cloud-aerosol relations [e.g., *Boucher and Lohmann*, 1995] led to AIF estimates ranging from

[1]Department of Atmospheric and Oceanic Science and ESSIC, University of Maryland, College Park, Maryland, USA.
[2]Department of Atmospheric Sciences, University of Texas A&M, College Station, Texas, USA.
[3]Also at Nanjing University of Information Science and Technology, School of Environmental Science and Technology, Jiangsu, China.
[4]Also at Pacific Northwest National Laboratory, Richland, Washington, USA.

0148-0227/08/2007JD008632$09.00

-1.1 to -4.4 Wm^{-2}, while the inversion methods constrained by global temperature records produced systematically lower values and narrower ranges in AIF (-1 to -1.9 Wm^{-2}). Which sets of calculations are more accurate is debatable [*Anderson et al.*, 2003], but it is indisputable that we must reconcile the two sets of estimations in order to better predict the climate change.

[4] Overestimation of AIF by the forward approach was conjectured based on a General Circulation Model's (GCM) overestimation of the rate of decrease in cloud particle size with aerosol optical depth relative to that from satellite observations [*Lohmann and Lesins*, 2002]. One explanation for the overestimation was that aerosols could have a warming effect by increasing the relative dispersion of the cloud droplet spectrum [*Liu and Daum*, 2002]. Incorporating this effect into a GCM reduces the magnitude of the AIF by 12 to 35% [*Rotstayn and Liu*, 2003], narrowing, but not bridging the big gap. Even if the gap is closed by a new mechanism, one cannot disregard the results obtained from backward calculations [*Anderson et al.*, 2003] unless past observations were proven erroneous or biased.

[5] The majority of previous studies on AIE concentrated on stratiform clouds formed in relatively dry regions/seasons or decoupled from the water vapor source [*Miller et al.*, 1998], as the Twomey effect is founded on the competition of water by cloud droplets. The parameterizations developed thereafter were likely skewed toward such conditions. It is important to realize that cloud droplet size is an "output" of a complex system, which involves interactions and feedbacks among aerosols, clouds, dynamics and thermodynamics. Derivation of the "partial derivative" between clouds and aerosols is thus a very challenging task, but it is critical for improving AIE estimates by models. In general, the AIE is veiled by a large variation in dynamic and thermodynamic conditions. To isolate and quantify the AIE, we need to develop "conditional AIE functions" to take into account different processes, as was attempted by *Feingold et al.* [2003]. To this end, we postulate and test a hypothesis that AIE is contingent upon atmospheric dynamics which may be delineated by cloud types, to the first order of approximation, and upon the atmospheric environment for which available water vapor amount is a key factor. Convective clouds developed in the summer over moist regions and stratus/stratocumulus clouds over dry regions or decoupled situations have distinct dynamic and thermodynamic settings. We selected both cumulus and marine stratiform scenes around the globe, with focused case-by-case analysis on the southeast United States (US) in the summer season.

[6] The following section describes the data sets used and section 3 describes the methodology followed in this study. Section 4 presents major findings. Potential artifacts are discussed and physical explanations are examined by means of model simulation in section 5. The study is summarized in section 6.

2. Data Sets

[7] The bulk of the data used in this study are from the Moderate Resolution Imaging Spectroradiometer (MODIS). MODIS provides an extensive remote sensing data set of aerosol, cloud, and atmospheric and surface variables over both ocean and land around the globe. The aerosol product (MOD04) includes aerosol optical depth (AOD) at three wavelengths: 0.47, 0.56, and 0.65 μm at a spatial resolution of about 10 km [*Remer et al.*, 2005]. The resolution is degraded from the original 1 km or less following several cloud screening tests [*Remer et al.*, 2005]. In our study, AOD at 0.56 μm is used as proxy of aerosol loading, which has its limitations while for our focus region AOD has been demonstrated to be quite a good proxy [*Hegg and Kaufman*, 1998]. The MODIS cloud products (MOD06) used in our study include cloud optical depth (COD), droplet effective radius (DER), liquid water path (LWP, a product of COD and DER), and cloud top temperature (CTT) [*King et al.*, 1992; *Platnick et al.*, 2003]. MOD06 has a spatial resolution of 1 km. Total column water vapor or 'precipitable water' (PW) was retrieved from the 0.94 μm channel [*Gao and Kaufman*, 2003] at 1 km. Level-2 granule data for aerosol, cloud and water vapor products are used in this study. In addition, the Level-1 sub-sampled reflectance product (at 5 km resolution) helps in choosing a case as explained in the methodology section. Level-1b 1km resolution radiance data are used to calculate brightness temperature (BT) as a proxy for cloud vertical development [*Rosenfeld and Lensky*, 1998].

[8] The multiangle imaging spectroradiometer (MISR) onboard the Terra satellite measures radiances in 4 spectral bands, at each of 9 viewing angles spreading out in the forward and aft directions along the flight path. AOD at 0.5 μm is retrieved over land and ocean using the radiances at these angles, and stored in the MISR level-2 aerosol product. It has a spatial resolution of approximately 16 km. The area coverage of MISR is smaller than MODIS because its swath width is 360 km compared to MODIS's 2330 km. The MISR AOD has been validated against AERONET ground observations [*Kahn et al.*, 2005] and proves to be of high quality over land.

[9] Geo-potential height, precipitable water and wind data from the National Centers for Environmental Prediction (NCEP) Reanalysis are used to depict the atmospheric circulation pattern over the study region. These daily reanalysis data have a spatial resolution of $2.5^\circ \times 2.5^\circ$. Over the center of our study region (the Gulf of Mexico), much observational data is assimilated into the reanalysis so the quality of the NCEP reanalysis data is relatively high.

3. Method and Regions of Study

[10] An ideal means of studying aerosol-cloud interactions would be to measure the properties of both quantities simultaneously. This is impossible for a passive remote sensing instrument like MODIS, as the cloud would block any signal from aerosols located beneath a cloud layer. This problem may be overcome/alleviated because aerosol properties are relatively homogeneous spatially compared to cloud properties, especially for cumulus clouds. We developed a 'semi-collocated and synchronized' technique to study the AIE for broken cumulus clouds. From the visible reflectance product (MOD02SSH), patches of broken cumulus clouds were first selected as our target scenes. The area of a target scene was chosen such that its coverage is large enough to include a statistically meaningful set of pixels and small enough to assure relatively homogenous dynamic and thermodynamic conditions. The

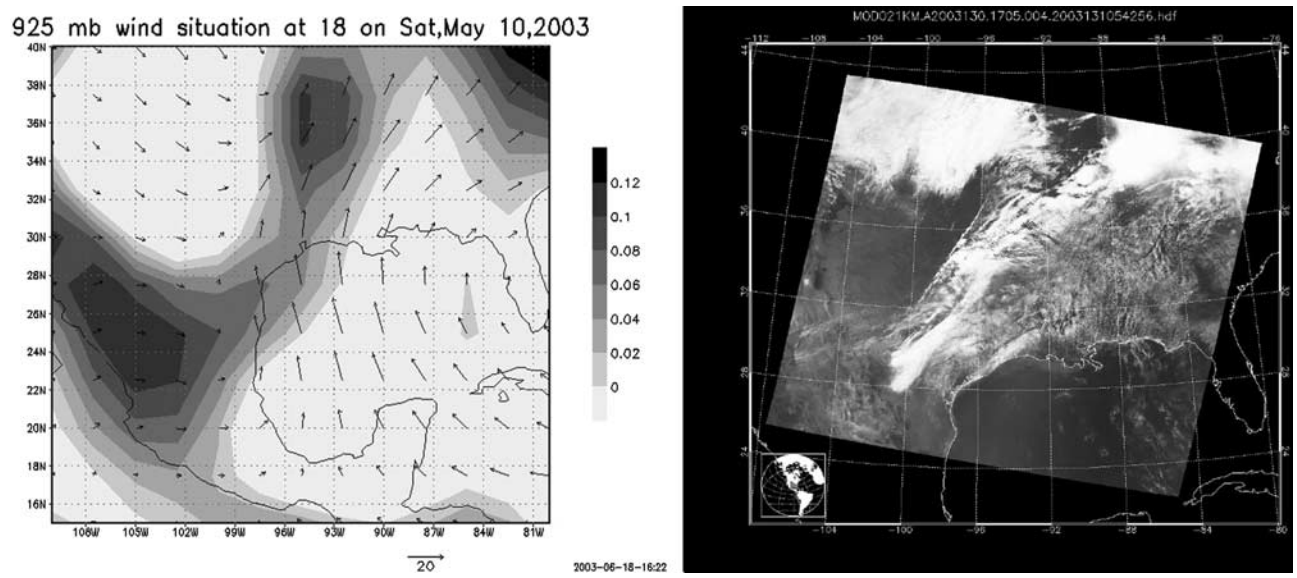

Figure 1. Right: MODIS cloud image at 17:05 UTC; Left: NCEP/NCAR reanalysis of wind vector (m/s) and vertical velocity (shaded area for updraft) at 18 UTC, both on 10 May 2003.

scenes selected usually encompass areas on the order of 10,000 km^2. Clear and cloudy pixels are collected for each 10-km by 10-km region over which one aerosol retrieval and up to 100 cloud retrievals are available. Mean cloud retrieval quantities are used here. It is worth noting that such cloudy scenes are not ideal from remote sensing point of view due to the three-dimensional (3-D) effects of clouds. We have taken various measures to minimize the effects, as explained later. On the other hand, use of cloud retrievals for large-scale more homogeneous cloud system would face a different challenge. Since no aerosol parameters can be obtained under cloudy conditions, previous AIE studies rely on cloud and aerosol data retrieved from cloudy and clear scenes that are far apart in time (e.g., a few days) and/or in space (e.g., hundreds of kilometers). As a result, the aerosol quantities used may not be representative of the cloudy scenes.

[11] We applied a set of screening criteria to these cloudy pixels to ensure data quality: (1) only highly confident overcast cloudy pixels, which is indicated by MODIS cloud mask, were selected; (2) COD is greater than 5 so that the uncertainty of cloud particle size and optical depth retrievals is reduced [*Nakajima and King*, 1990]; (3) only water clouds are considered because ice particles have very different properties from water droplets and low clouds topped with cirrus are excluded by applying a criteria of cloud top pressure larger than 600mb and cloud phase being water as indicated in cloud product; and (4) DER retrievals less than 4 and larger than 28 are considered problematic and discarded. With these criteria and the fact that precipitation associated with convective cumulus clouds occurs often in late afternoon, precipitating clouds, if any, are unlikely to distort our statistics. PW data were retrieved from nearby clear pixels to represent column-integrated water vapor. For each aerosol retrieval over a 100 km^2, retrieved cloud quantities (DER, COD and BT) were averaged for all cloudy pixels, and a mean PW was obtained by averaging the PW data from all clear pixels in a scene. Quasi-coincident aerosol and cloud data were thus created. It ensures that measurements for aerosol and cloud properties are close enough to each other. Over such a small scale, aerosols and clouds are more likely to interact. On the other hand, the retrievals could be contaminated, leading to a potential artifact that will be addressed later.

[12] Over our focus region of eastern US, the AIE is studied case-by-case by correlating aerosol and cloud quantities, following the conventional method but applied over much smaller areas with simultaneous aerosol and cloud observations. Our basic assumption is that for each case, the general environmental conditions remain identical across that area, effectively reducing the impact of large scale meteorology. The relationships retrieved thereafter would be a signal of AIE, which has certain superiority over those derived from clear and cloudy scenes far apart in time and/or space. Correlation analyses were done among multivariables: AOD, COD, DER and PW.

[13] To study the aerosol effect on cumulus clouds formed under conditions where water vapor amount is variable, we chose a transect from southeastern US to northeastern US as our focus region. Abundant convective clouds form over land surrounding the Gulf region during summer and the water vapor amount varies considerably from the coast to inland. Water vapor is blown inland from the ocean by the winds created by the prevailing Bermuda high-pressure system and the local ocean sea breeze in summer. Land surface heating generates sufficient convection to fuel cumulus cloud development. The interaction between cloud microphysics and aerosol for locally generated clouds is expected to differ considerably from that of clouds transported from elsewhere by a front or other large-scale weather systems.

[14] Figure 1 shows the distribution of a convective cloud scene, which contains two cloud regimes: sea-breeze-induced small-scale convective clouds in the south and a frontal meso-scale cloud system driven by large-scale atmospheric circulation in the north. It is the former cloud type that is investigated in this study. We have browsed through a number of MODIS images taken during July of 2001.

[15] We extend our analysis to other regions over the globe like the Indian subcontinent, Eastern China, the

Table 1. Regions Selected for Global Analysis[a]

Region	Latitude range	Longitude range	Dominant Aerosol/Cloud Types	Period	AIE efficiency	Sample size
North Atlantic	10–20N	20–40W	Dust, Stratocumulus	June–August, 2002	Negative	99,978
South Atlantic	5–20S	5E–20W	Smoke, Stratocumulus	June–August, 2002	Negative	100,377
Southern Pacific	5–25S	75–105W	Sea salt, sulfate and pollution, Stratocumulus	August–October, 2002	Negative	74,216
Indian Ocean	12–20N	60–70E	Dust with pollution, Trade cumulus	June–August, 2002	Negative	94,023
India	13–24N	70–85E	Mixture of sulfate, dust, sea salt and smoke, cumulus	June–August, 2002	Neutral	53,888
Amazonia	8S–12N	44–76W	Mainly smoke	August–October, 2002	Negative	672,421
Southeastern China	23–43N	100–120E	Mixture, cumulus	June–August, 2002	Positive	179,533

[a]The location, dominant aerosol and cloud types, times the AIE efficiency and sample sizes are given.

Amazonia, Northern and Southern Atlantic, Southeastern Pacific, and Indian Ocean as summarized in Table 1. Cloud types over these regions encompass fair-weather cumulus, marine stratiform clouds and trade cumulus; aerosols are also diverse, including sulfate, dust, sea salt, smoke, organics and mixture of them. The wide spectrum of cloud and aerosol types covered in the analysis offer an opportunity to both investigate the variation of AIE and gauge our analysis against previously well-established results over regions like Brazil and Indian Ocean. Consistency/inconsistency is a further test of the validity of our analysis method, data and results. For each region we use the same technique to select and filter the data, and combine the filtered data points together to gain enough samples to get stable statistics. Data were stratified in each region in terms of environmental variables like water vapor amount, viewing geometry etc to

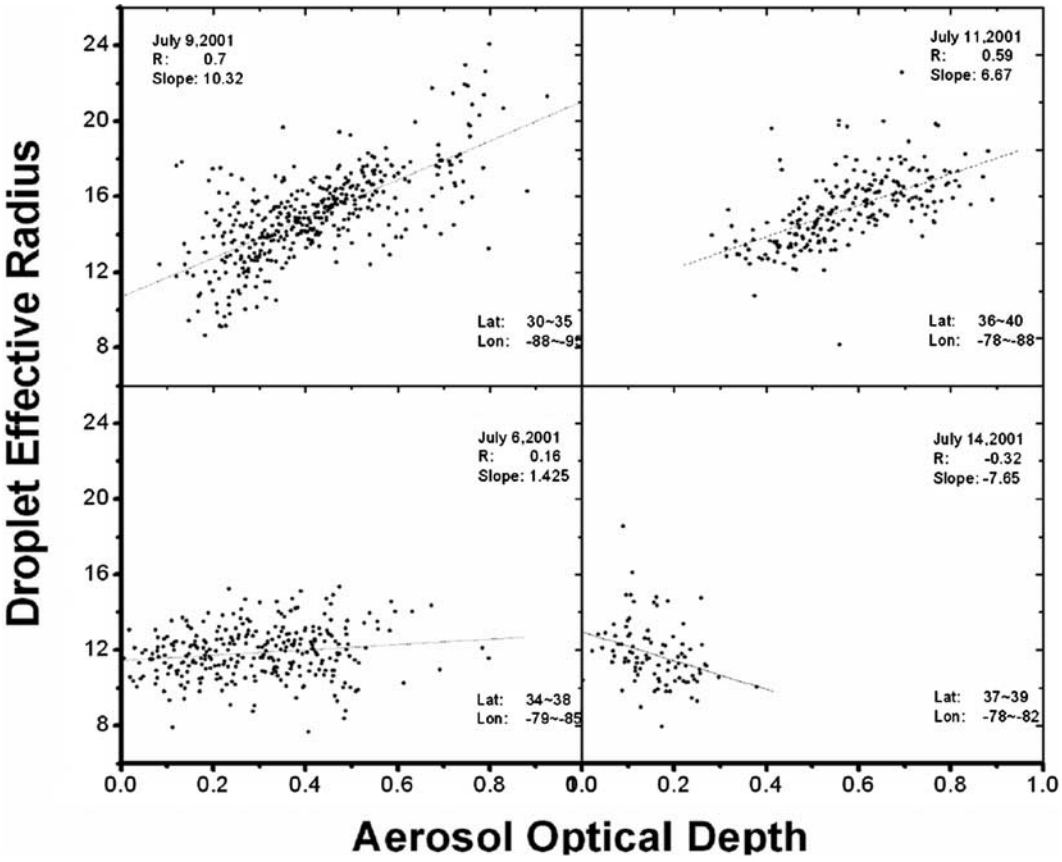

Figure 2. AIE efficiency for four cases. The time and location, correlation coefficient (R), and the slope of each case are provided in each panel.

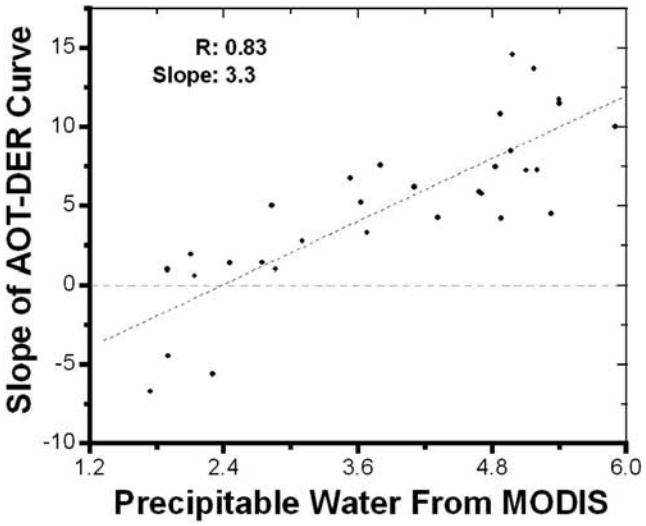

Figure 3. Dependence of the AIE efficiency on precipitable water (cm/m^2) for all cases studied in southwest and interior US (see Figure 5). The correlation coefficient (R) and slope between these two quantities are given. The unit for precipitable water is in centimeters.

suppress large scale influence. For each stratified sub-set, the data are binned into three equal-size groups based on their AOD values, for which BT-DER profiles [*Rosenfeld and Lensky*, 1998] are calculated and the AIE is examined as the difference among profiles that have distinct aerosol loadings. We use *student*'s *t*-test to examine the significance of the difference.

4. Results From Focus Region

[16] AOD-DER plots of four representative cases are presented in Figure 2. The slope of the AOD-DER relationship can be interpreted as the change of DER for a unit change of AOD and here it is referred to as the AIE efficiency. Like previous findings, the AIE efficiency varies considerably, but they can be either negative or positive in our study, ranging from −7.7 to 12. The majority of cases we examined have a positive AIE efficiency, which means that the cloud droplet size increases with increasing loading of aerosols. This is a different result from earlier studies and could imply a different physical process governing the AIE for cumulus clouds relative to stratiform clouds, barring the presence of retrieval artifacts inherent to remote sensing. Potential artifacts are investigated below.

[17] PW was once hypothesized as a factor dictating the variation of AIE [*Kaufman and Fraser*, 1997], but it was later negated for smoke aerosols observed during the dry season in the Amazon [*Feingold et al.*, 2001]. This may imply that the different sensitivities have something to do with aerosol hygroscopic properties. Along the corridor from Texas to the Northeast US (our US study region), industrial emissions and sea salt (near the coast) are dominant, while elemental and organic carbon fractions are more plentiful in Mexico. Other factors have also been hypothesized such as cloud type, dynamics, turbulence, and aerosol properties, or their combinations [*Feingold et al.*, 2001] but few have been confirmed with real observational data. Close correlation was found between the AIE and vertical turbulence measured by an aircraft [*Leaitch et al.*, 1996]. Using a cloud parcel model, *Feingold et al.* [2003] found that changes in DER with aerosol extinction have a strong dependence on updraft for high aerosol loading conditions.

[18] To find factors that influence the AIE efficiency in our study, a set of statistical analyses were performed. PW turns out to be the most influential factor in driving the variation of AIE efficiency as demonstrated in Figure 3. Each point in Figure 3 represents a case corresponding to a cumulus cloud scene. The correlation coefficient between AIE efficiency and PW is as high as 0.84. In other words, about 70% of the variance of AIE efficiency is explained by changes in PW. The AIE efficiency is positive and large for moist regions and small, or negative, for dry regions. This relationship is also clearly seen from a map showing the spatial variation of the AIE efficiency and the distribution of mean PW averaged over July 2001 for our study region (Figure 4).

5. Discussions and Possible Explanations

5.1. Artifact Explanations

[19] Caution is warranted in accepting the above finding in light of various data uncertainties. A critical question is whether the dependence of DER on AOD and its slope on PW result from observational artifacts. If an error in one variable is correlated with an error in another, a false correlation may occur between the two quantities. Even if the two quantities had no retrieval errors, they could be physically linked to a third factor, leading to an ''apparent'' or false correlation. We examined all potential third factors including cloud contamination, aerosol humidity effect, cloud dynamic effect and 3-D effects that could explain the observed correlation.

5.1.1. Partially Cloudy Effect

[20] MODIS aerosol algorithm has a strict cloud masking procedure to ensure that only clear pixels are retrieved [*Remer et al.*, 2005]. It uses spatial variability to identify low clouds [*Martins et al.*, 2002] and 1.38 μm channel [*Gao et al.*, 2002] to detect high clouds in addition to standard cloud mask product. It also excludes the 50% brightest pixels and the 20% darkest pixels for possible cloud contaminations including both the scattering and shadowing effects of broken clouds. Nevertheless, some cloud-contaminated pixels might still be erroneously identified as clear. Meanwhile, reflected radiance from partially clear pixels may be accentuated due to cloud scattering and reflectance, leading to overestimation of AOD. Also a partial cloudy pixel can result in the overestimation of DER due to lowered reflectance at the 2.1 μm channel [*Nakajima and King*, 1990]. Thus the co-existence of partially cloudy and partially clear scenes could incur a false correlation between DER and AOD.

[21] Several tests were conducted to assess the potential effect of partially cloudy scenes. First, correlations between cloud fraction and AOD and DER are calculated to determine the impact of cloud fraction on both retrievals. No significant correlations were found between AOD/DER and cloud fraction in our study. The correlation coefficients

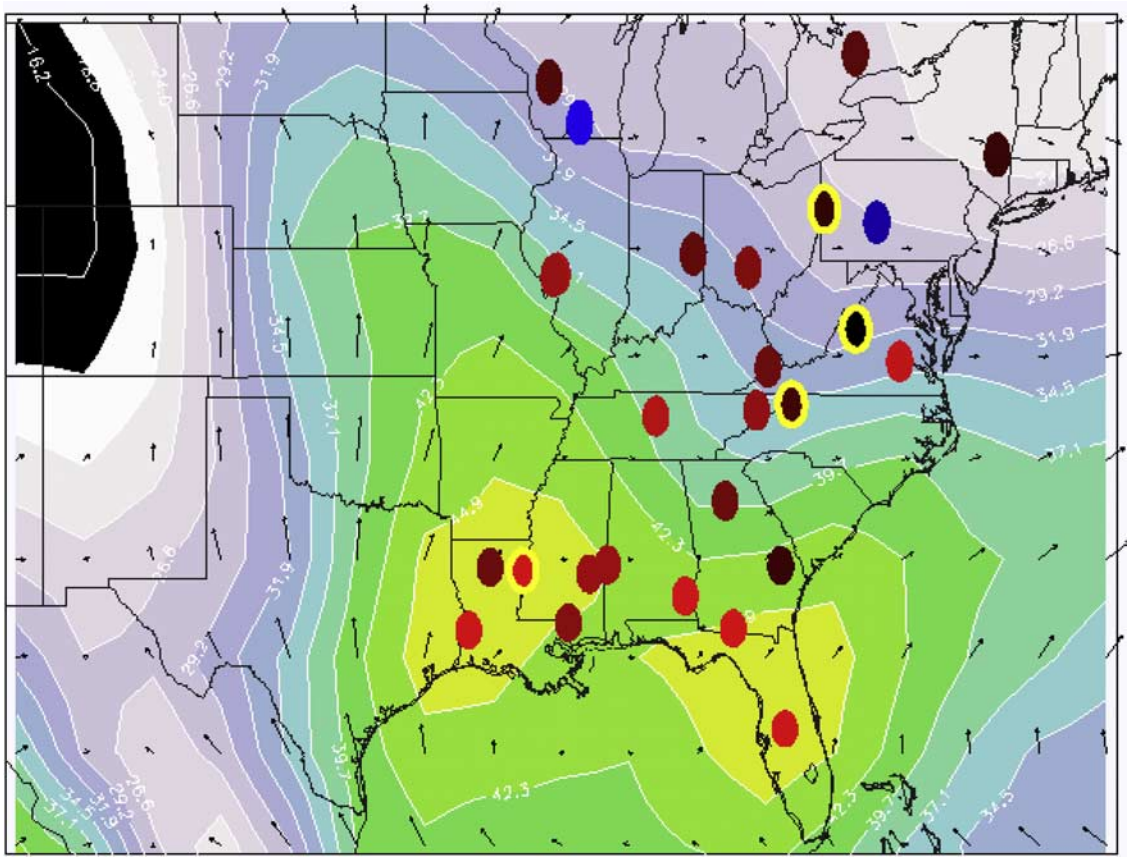

Figure 4. Distribution of the locations for the scenes selected in the study. Bright red dots denote large slopes, darker red for smaller slopes and blue for negative slopes. Monthly mean precipitable water and wind vectors from the NCEP-NCAR reanalysis are superimposed. The yellow circles are the four cases presented in Figure 2.

between cloud fraction and AOD for the four cases shown in Figure 2 are 0, 0.05, 0.26, and 0.05. To further examine the effect of cloud fraction, the data were stratified by cloud fraction and the AOD-DER slopes were determined for high, greater than 20%, and low, between 0% and 10%, cloud fractions. As plotted in Figure 5a and 5b, the two slopes are almost identical to each other and the mean values of AOT and DER for these two sub-data sets are also identical. Secondly, clusters of cloudy pixels were identified that are connected to each other. Inside a 10 km by 10 km

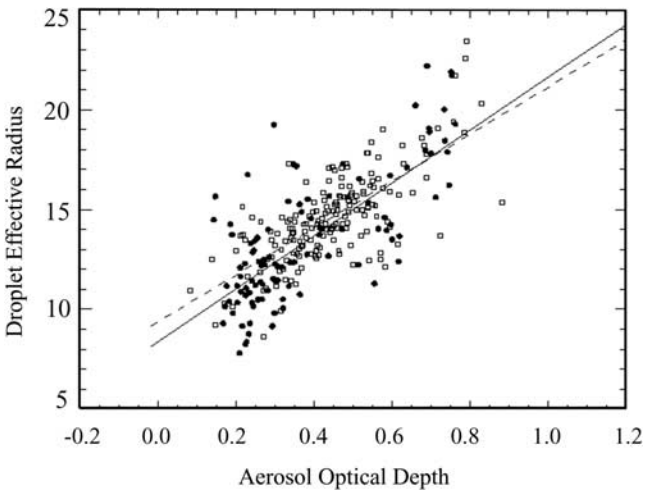

Figure 5a. AOD-DER plots using pixels classified by cloud fraction. Solid line is for cloud pixels at the lower end of cloud fraction distribution and the dashed line is for those at the higher end of cloud fraction distribution.

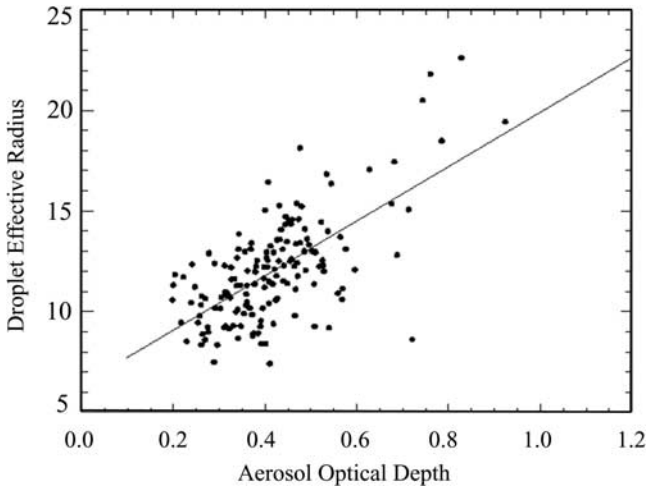

Figure 5b. The AOD-DER correlation using only cloudy pixels with connectivity equal 8.

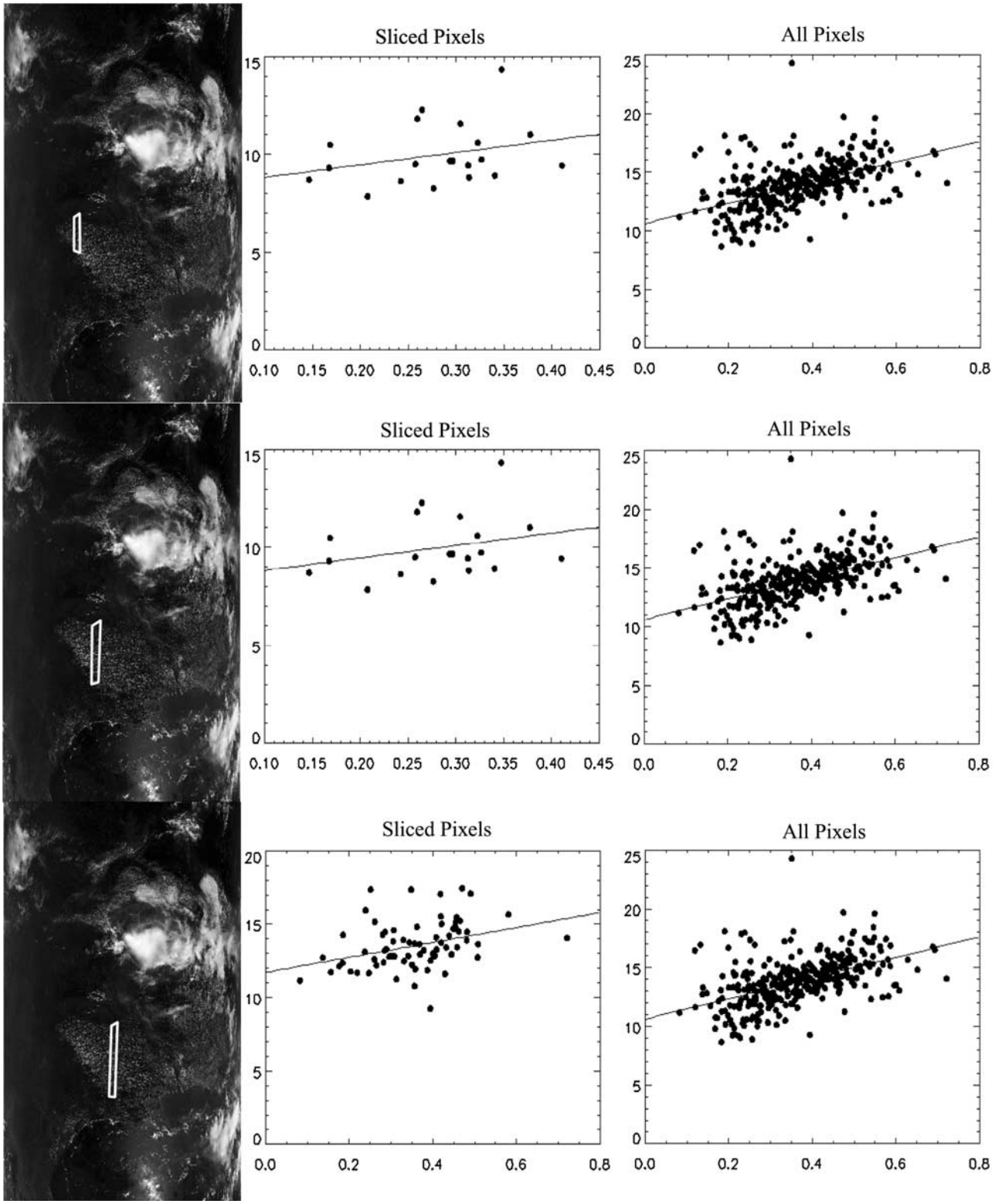

Figure 6. Three slices of a convective cloud scene (red polygons on left images) at 1900 UTC on 9 July 2001 and associated AOD-DER plots (middle panels), in comparison with the AOD-DER plots for the entire scene (right panels).

aerosol pixel, the number of clusters is an indicator of the 'brokenness' of clouds. The data were then stratified and the AOT-DER relationships were analyzed corresponding to different numbers of clusters. Nearly identical slopes were obtained for the data with a higher number of clusters, 3 to 5, and lower, 2 to 3 (Figure not shown here). Connectivity of a cloudy pixel is defined by the number of cloudy pixels that are directly connected to it. If a cloudy pixel is

surrounded by all immediate neighboring cloudy pixels, the connectivity is equal to 8 and this pixel is less likely to be partially cloudy than those with a low number of connectivity. An AOD-DER analysis for the data with connectivity equal to 8 showed a similar slope to the plot in Figure 5b that includes all possible pixels. From the analyses, we may conclude that the partially cloudy effect is not likely the cause of the observed relationship, at least not a major one.

5.1.2. Cloud 3-D Effect

[22] The cloud retrieving algorithms that were used to produce the MODIS cloud products (MOD06) assume plane-parallel clouds [*Nakajima and King*, 1990]. For 3-D shaped clouds, variations in the satellite viewing geometry (relative to the Sun's position) can change satellite-measured signals and incur errors in the retrievals of both aerosol and cloud properties as discussed in depth by *Vant-Hull et al.* [2007] and *Wen et al.* [2006]. If a satellite sensor and the sun are on the same side relative to the nadir, a portion of the incoming solar radiation is reflected by the cloud side and larger radiances are measured. Across a swath of a satellite image, the viewing geometry varies from backward to forward scattering directions, or vice versa, depending on the spacecraft orbits, namely local morning or afternoon. *Vant-Hull et al.* [2006] noted that the relative azimuth angle (RAA) between satellite and the sun is a key parameter determining the retrieval biases. To minimize the influence of this cloud 3-D effect, we selected narrow image slices in north-south directions so that the RAA remains virtually identical. For nearly all cases studied, the correlation slopes between AOD and DER for the sliced scenes are in agreement with those derived using all pixels, while the magnitudes of the slopes may differ somewhat, as shown in Figure 6. The slight deviation in the magnitude could result from sampling errors, as data samples are fewer for sliced scenes than for the overall scenes. The variations in the slope may also be a manifestation of the 3-D effect, but the persisting general agreements seem not to support the suggestion that the cloud 3-D effect is the major cause for a false correlation between AOD and DER. Further evidence against 3-D effect will be presented below.

5.1.3. Swelling Effect of Water Vapor

[23] Aerosols can be divided into two categories according to their hygroscopicity. Hygroscopic aerosols grow in size when soaking up water vapor and deliquesce when the humidity passes their 'deliquescence relative humidity' [*Hanel*, 1976]. Hydrophobic aerosols do not change much in size with humidity. It has been reported that AOD increases in response to both size and refractive index changes due to water vapor swelling [*Feingold et al.*, 2003]. Suppose aerosols around deeper clouds, for example, swell more because of higher relative humidity and thus have a larger optical depth. At the same time, deeper clouds tend to have larger droplets than shallower clouds. A positive correlation may thus be observed between aerosol loading and cloud droplet size even with perfect retrievals of the two quantities.

[24] For aerosols over the Southern Great Plains, *Sheridan et al.* [2001] showed that hygroscopic growth is an important factor in determining the aerosol optical depth for sea salt aerosols. Using aircraft and lidar data from the Atmospheric Radiation Measurement program (ARM), a positive correlation between humidity and aerosol extinction was observed [*Jeong et al.*, 2007]. Precipitable water is used here to check the swelling effect. In our analysis, we do observe some degree of correlations between DER and AOD and PW, as seen in Figure 7. However, the correlations are too weak to explain the tight correlation between AOD and DER. The weak correlation between AOD and PW might have something to do with the fact that the variability of AOD itself often is large and hence can outweigh the effect of humidity. Therefore the humidity effect cannot explain the AIE.

5.1.4. Dynamic Effect

[25] There is another scenario under which higher aerosol loading may be anticipated, namely, the ''pumping effect''. Stronger convection produces deeper clouds. For convective clouds during the developing stage, deeper clouds tend to have larger droplets at cloud tops. In situ aircraft measurements in the Amazon showed a clear dependence of DER on the height above the cloud base (personal communication with V. Martins at NASA/GSFC). Meanwhile, convergence accompanying updrafts and detrainment of particles by clouds can 'pile' up aerosols around clouds. Both scenarios result in a false correlation between AOD and DER, which is referred to here as the 'dynamic effect'. On the other hand, as postulated by *Young* [1993], aerosols not only impact directly on cloud microphysics but also affect the dynamics through modification of radiative and thermodynamic heating. Locally generated cumulus clouds are formed from rising thermals containing aerosols that serve as CCNs. Interaction between aerosols and cloud development is thus likely to take place under these circumstances. Therefore the correlation can be a manifestation of the interaction between aerosol and cloud.

[26] To get a first glance of the potential dynamic effect, we assume that clouds have a uniform cloud base height over the relatively small study region. CTT is then a proxy for cloud depth. In either scenario, a negative correlation would be expected between CTT and DER, and between CTT and AOD, which appeared to be true for some cases. To check if cloud dynamic effects are the cause for the correlation between AOD and DER, the two variables were analyzed with the condition that the CTT fall within very narrow intervals (1 degree) (Figure 8). Suppose the dynamic effect is the sole cause for the correlation observed, we would observe no positive correlation. However, the same positive correlation between AOD and DER exists for the sliced sub-samples, which suggests that the dynamic effect is not the sole cause for AOD-DER correlation.

5.1.5. Surface Effect

[27] Retrieval of AOD over land is much more challenging than over oceans, due to the influence of the surface. The retrieval uncertainty is significantly smaller over ocean than over land [*Remer et al.*, 2005]. Prior to MODIS, most global aerosol products were confined to oceans [*Nakajima and Higurashi*, 1998]. AOD-DER correlation analyses were performed using data collected over the ocean to check if the correlation is unique to land. Many cases of positive correlations were found and an ensemble analysis done over the Caribbean Sea also reveals positive AIE efficiency (not shown here). This may imply AIE's dependence on cloud regime and aerosol type, which is further explored in our global analysis below. It has also been shown in previous

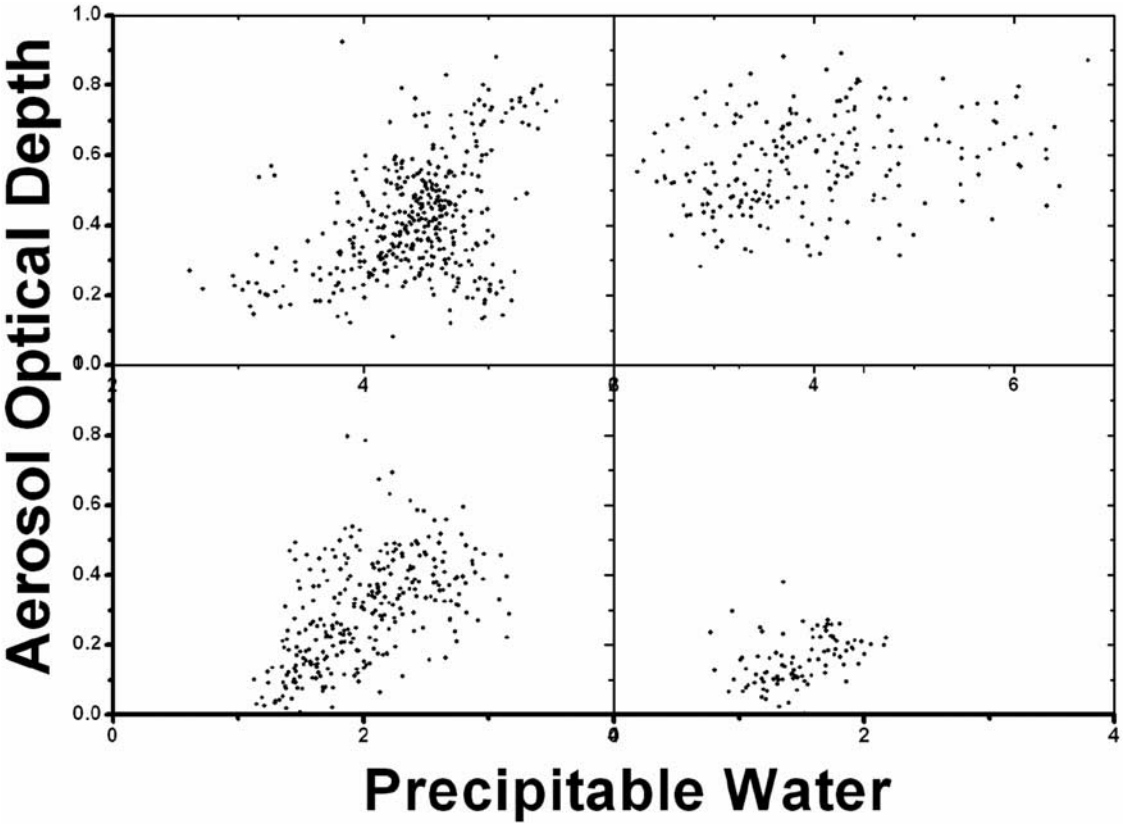

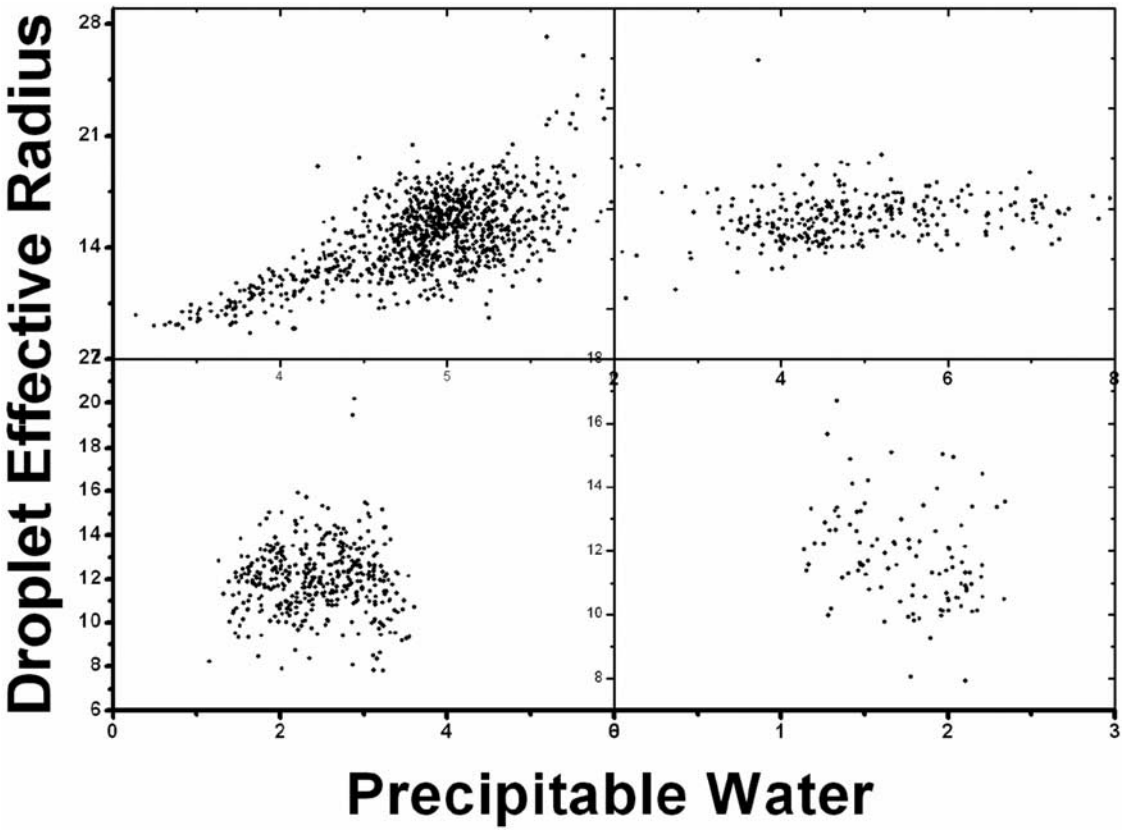

Figure 7. (a) Dependence of aerosol optical depth data on precipitable water amount for the same four cases as in Figure 2. (b) Dependence of droplet effective radius on precipitable water for the four cases as in Figure 2.

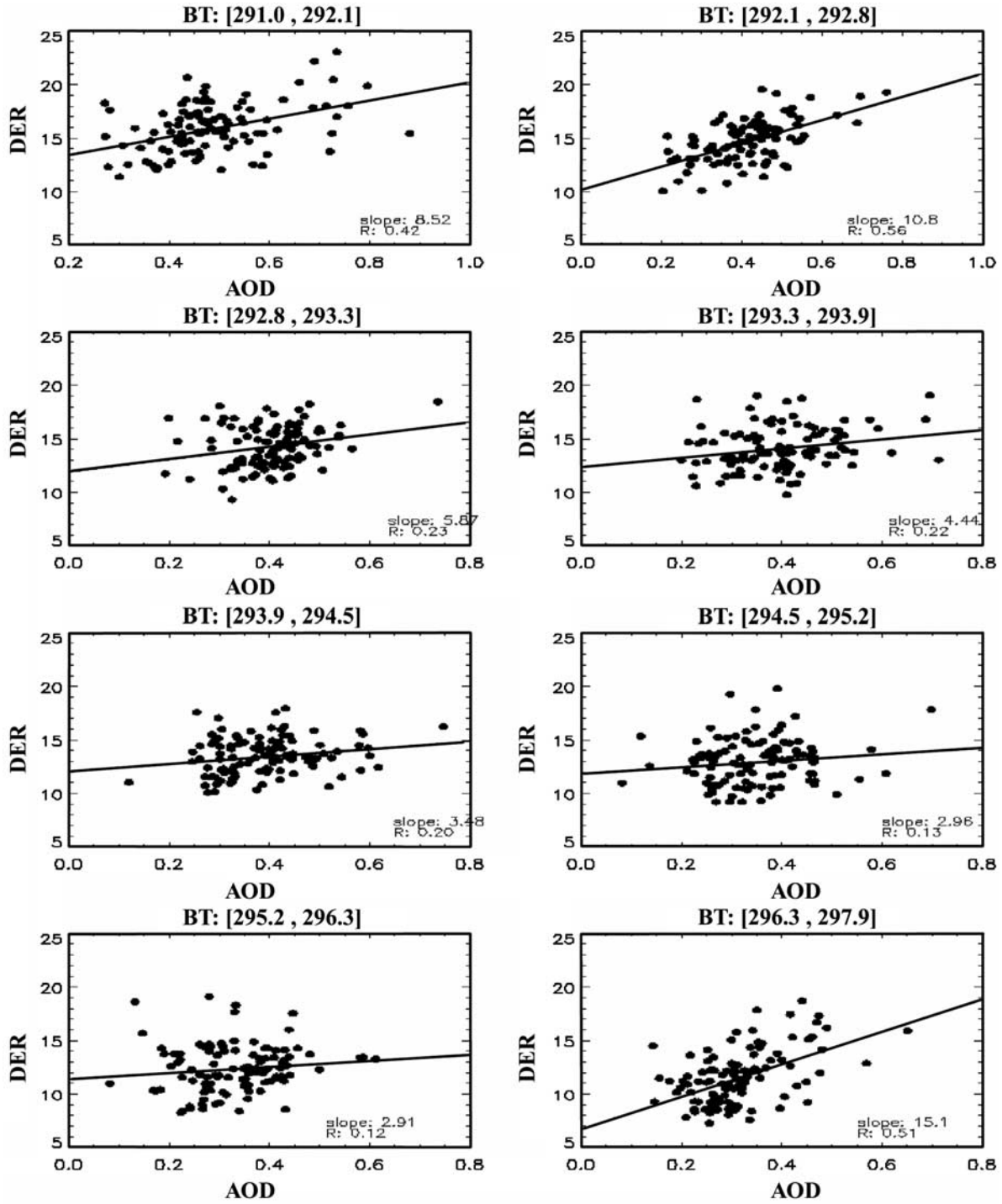

Figure 8. AOT-DER plots for eight intervals of cloud top temperature for a case at 1900 UTC on 9 July 2001. The intervals of temperature are provided in the plot titles.

studies that different cloud types have different susceptibility to aerosols [*Platnick and Twomey*, 1994].

[28] A fixed relation between surface albedo at 2.1 μm and visible channels is assumed for AOD retrievals over land [*Kaufman et al.*, 1997]. This method is sound in general [*Kaufman et al.*, 2002] with a potential exception over wetland surfaces where the correlation established for global applications may have systematic errors. Since thermally induced cumulus clouds are more likely to occur over wetter than drier areas, a false correlation between AOD and DER might exist. Unfortunately, we cannot address the issue directly. An indirect approach was pursued using MISR AOD data. The principle of AOD retrieval from MISR is very different from the MODIS AOD retrieval. The former is based on changes in atmospheric scattering from different viewing angles, which is much less sensitive to errors in surface albedo [*Kahn et al.*, 2005]. Within the narrower strips of MISR images, MODIS and MISR instru-

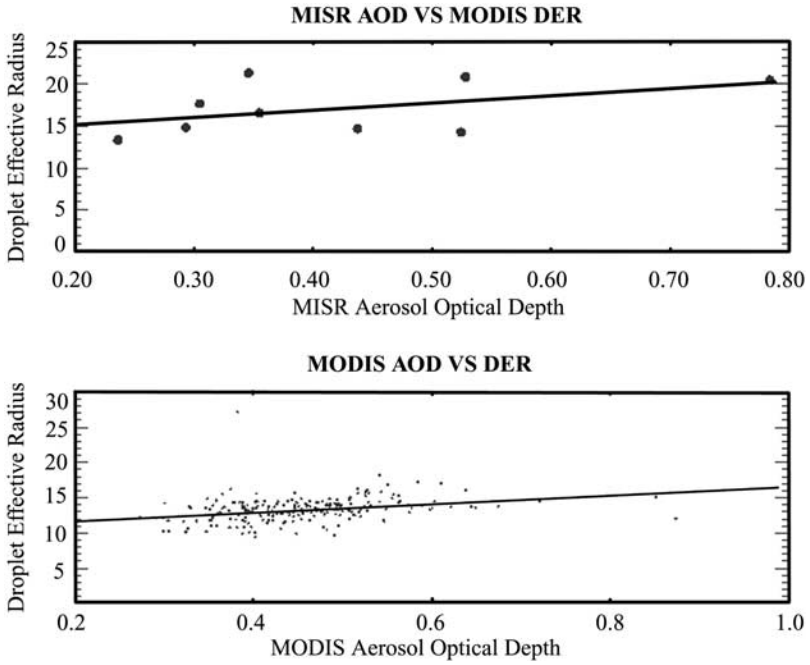

Figure 9. Collocated MISR (upper) and MODIS (lower) AOT-DER plots for a case at 1835 UTC on 6 July 2001.

ments deployed on the Terra platform observe the same aerosol field. There are much less coincident MISR AOD and MODIS DER data due to spatial coverage differences and more importantly, differences in the retrieval algorithms, especially the cloud masking procedure. Nevertheless, for all the cases we analyzed, similar trends and slopes, though much worse correlation, between MISR AOD and MODIS DER were found, as seen in Figure 9. This implies that the surface effect is not a dominant factor.

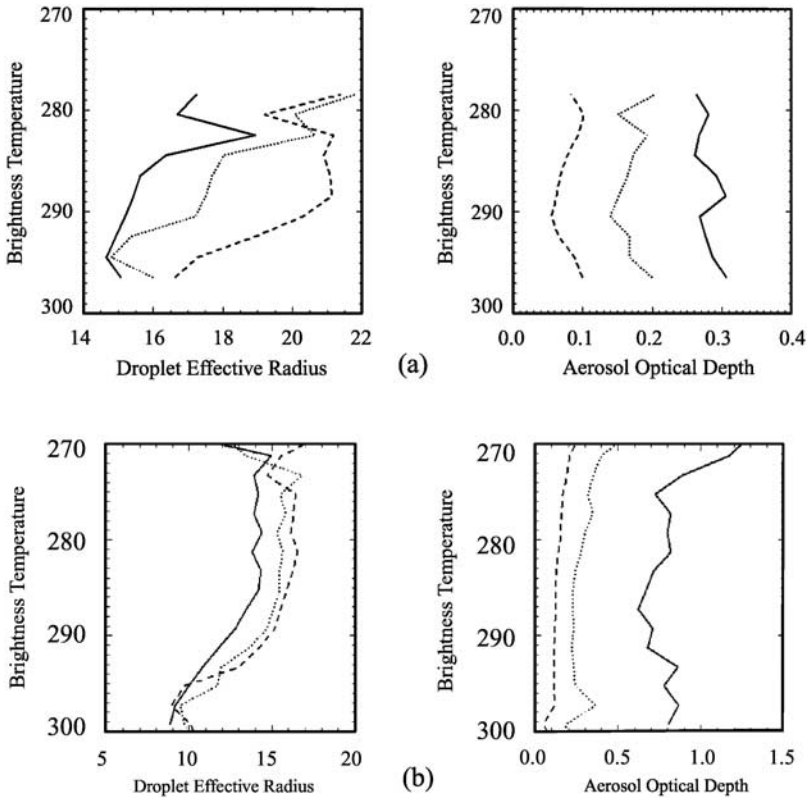

Figure 10. (a) BT-DER profiles for trade cumulus over Indian Ocean; (b) BT-DER profiles for fair-weather cumulus over Amazonia.

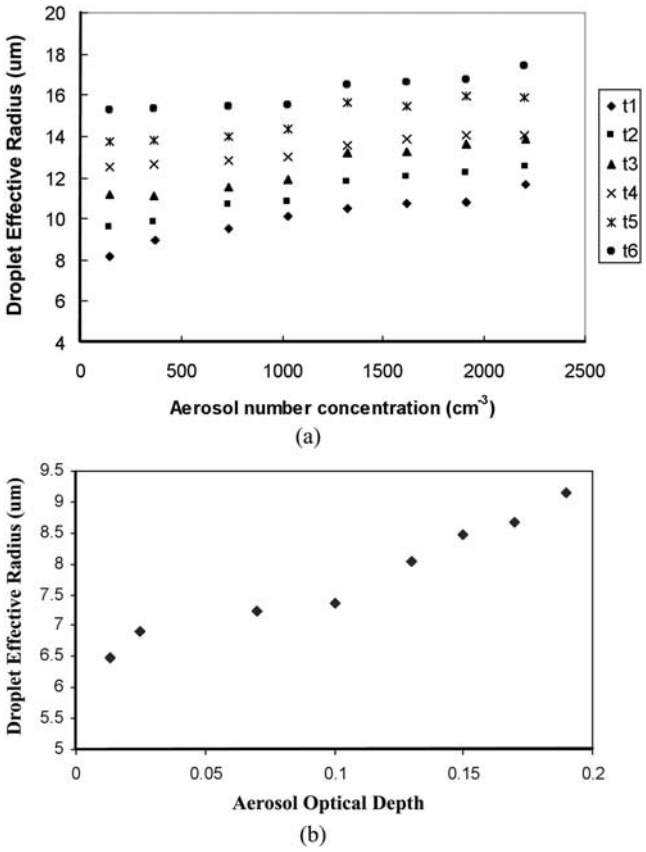

Figure 11. (a) Cloud droplet effective radius versus aerosol number concentration at varying time intervals increasing from t1 to t6 with a 5 min step, (b) Cloud droplet effective radius versus aerosol optical depth at t1 (integration time 210 min). All the values indicated in the figure were averaged over the selected domain.

5.2. Possible Physical Mechanisms

[29] The various analyses presented above lead to a sound argument that the observed positive relation between DER and AOD is likely a real phenomenon. This is further reinforced by analyzing more aerosol and cloud data over several other regions around the world as is presented below. We present two plausible mechanisms to explain the observed relationship, one regarding to aerosol composition, which is an important factor in determining the activation of droplets [*Facchini et al.*, 1999], and the other to the existence of giant CCNs.

5.2.1. Global Analysis

[30] Our investigations of the various potential artifacts are extensive while we note that there still could be other unrecognized and/or unverifiable possibilities. An alternative means to verify the validity of our results is to compare them with any established results and to test the null hypothesis that our observed relation is simply a result of certain artificial correlation. Field campaigns and in situ measurements have been made to study AIE over Amazonia [*Kaufman et al.*, 1992, 1998; *Andreae et al.*, 2004] and Indian Ocean [*Ramanathan et al.*, 2001]. For both regions, our analyses agree with the past finding that DER decreases with AOD as in Figure 10. Among other global analyses (summarized in Table 1), negative AIE efficiencies are also detected for regions with extensive stratocumulus clouds like Southeastern Pacific and Atlantic, where previous studies also showed negative AIE efficiencies. Among the regions we analyzed, only southeastern US and southeastern China show dominant positive AIE efficiency while India shows nearly no dependence of DER on AOD. The differences of DER for different aerosol loadings are mostly significant at level 95% or higher, except for Indian where no discernible changes occur as aerosol loading changes. As indirect evidences, these results lend us more confidence that the observed positive AIE efficiency is likely to be real. The null hypothesis that the observed relation is due to artificial correlations is effectively negated because if the phenomenon simply resulted from an artifact, we would see it everywhere for the same kind of clouds.

[31] However, we recognize the similar atmospheric circulation patterns in southeastern China and US with a high pressure system sitting off the coast. The similarity may imply that the origin of the air mass may have strong influence on the cloud development and thus AIE, which has been noted by *Brenguier et al.* [2003]. There are various pathways through which cloud properties are affected by the origin of air mass but there seems to be no direct link with the positive AOD-DER relation as found in this study. As such, we propose the following two plausible mechanisms.

5.2.2. Aerosol Composition

[32] In the southeast of Texas, oxidation of volatile organic compounds (VOCs) from industrial and transportation sources contributes significantly to formation and growth of aerosols [*Zhang et al.*, 2004; *Fan et al.*, 2006]. Aerosol composition is an important factor to affect the activation processes, especially for aerosols containing low solubility organics [*Laaksonen et al.*, 1998; *Shantz et al.*, 2003; *Fan et al.*, 2007]. The organics are the major aerosol components in Houston area as shown in the observational and modeling studies of *Russell et al.* [2004] and *Fan et al.* [2005]. Those organics are generally considered to be slightly soluble with very low solubility of about 0.001 kg/kg (of water) set in our simulations [*Fan et al.*, 2007], so-called slightly soluble organics (SSO). With increasing content of SSO, the low solubility increases the critical supersaturation, resulting in less activated particles as noted by *Broekhuizen et al.* [2004] and *Shantz et al.* [2003]. In order to include the effect of slightly soluble substances, the Köhler theory has to be reformulated to calculate CCN activation, which has been described in detail by *Laaksonen et al.* [1998]. This reformulation of Köhler theory to include the effect of SSO has been incorporated in a 2-D Goddard Cumulus Ensemble model (GCE) with a spectral-bin microphysics [*Tao et al.*, 2003] and the results have been validated by the observed cloud properties in Houston [*Fan et al.*, 2007]. This revised cloud-resolving model is employed here to investigate the impact of changing SSO on cloud microphysics over southeast of Texas and Galveston Bay near the Gulf of Mexico. Details of the model configurations are described by *Fan et al.* [2007]. Eight simulations were performed, in which total aerosol concentration was assumed to increase from 150 to 2200 cm^{-3} gradually. The content of SSO was also assumed to increase with total aerosol concentration.

[33] Simulations were performed based on a sounding on 24 August 2000 at 7:00 am (local time) from Lake Charles

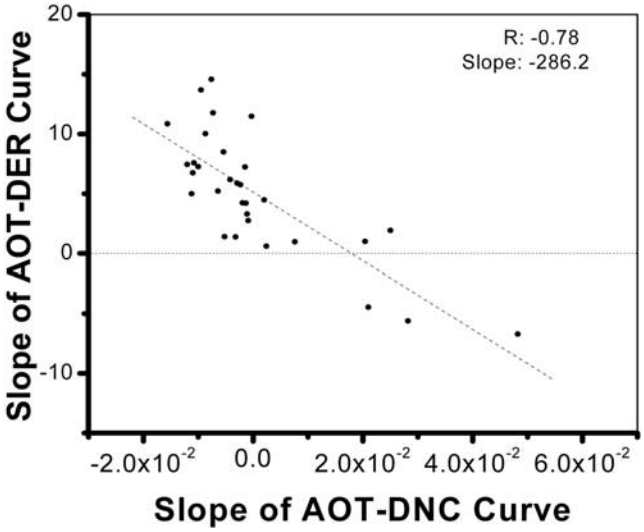

Figure 12. The relation between AIE coefficients and slopes of AOT-DNC for all cases. The correlation coefficient and the slope are provided with legend in the plot.

(93.21W, 30.11N). The vertical temperature and dew point profiles revealed an unstable atmosphere with convective available potential energy (CAPE) of 1800 J kg^{-1}, integrated from the level of 500 m. The surface temperature was about 26°C and the surface relative humidity was high up to 87%. The observed surface fluxes were imposed to initiate the convection. The horizontal resolution was 0.5 km (test runs with 250 m do not change our results). The stretched vertical resolution was used with 28 m for the lowest layer. Shallow cumulus clouds were generated at about 210 min. Figure 11 presents the relationship between the cloud DER and the aerosol number concentration (Figure 11a) and AOD at 0.55 μm (Figure 11b) for eight simulations. The different colors in Figure 10a denote the different stages of cloud evolution with an interval of 5 min from the beginning of cloud formation. The clouds simulated are warm cumulus of no precipitation. DER increases with both aerosol concentration and AOD. It becomes less pronounced with the evolution of clouds. The increases originate from a decreasing number of activated aerosols with an increasing SSO content. The low solubility of SSO acts to the increase of the critical supersaturation for particles to be activated since the solution term is getting smaller, resulting in less activated particles and thus smaller droplet number concentration (DNC). In our simulation the positive AIE efficiency only

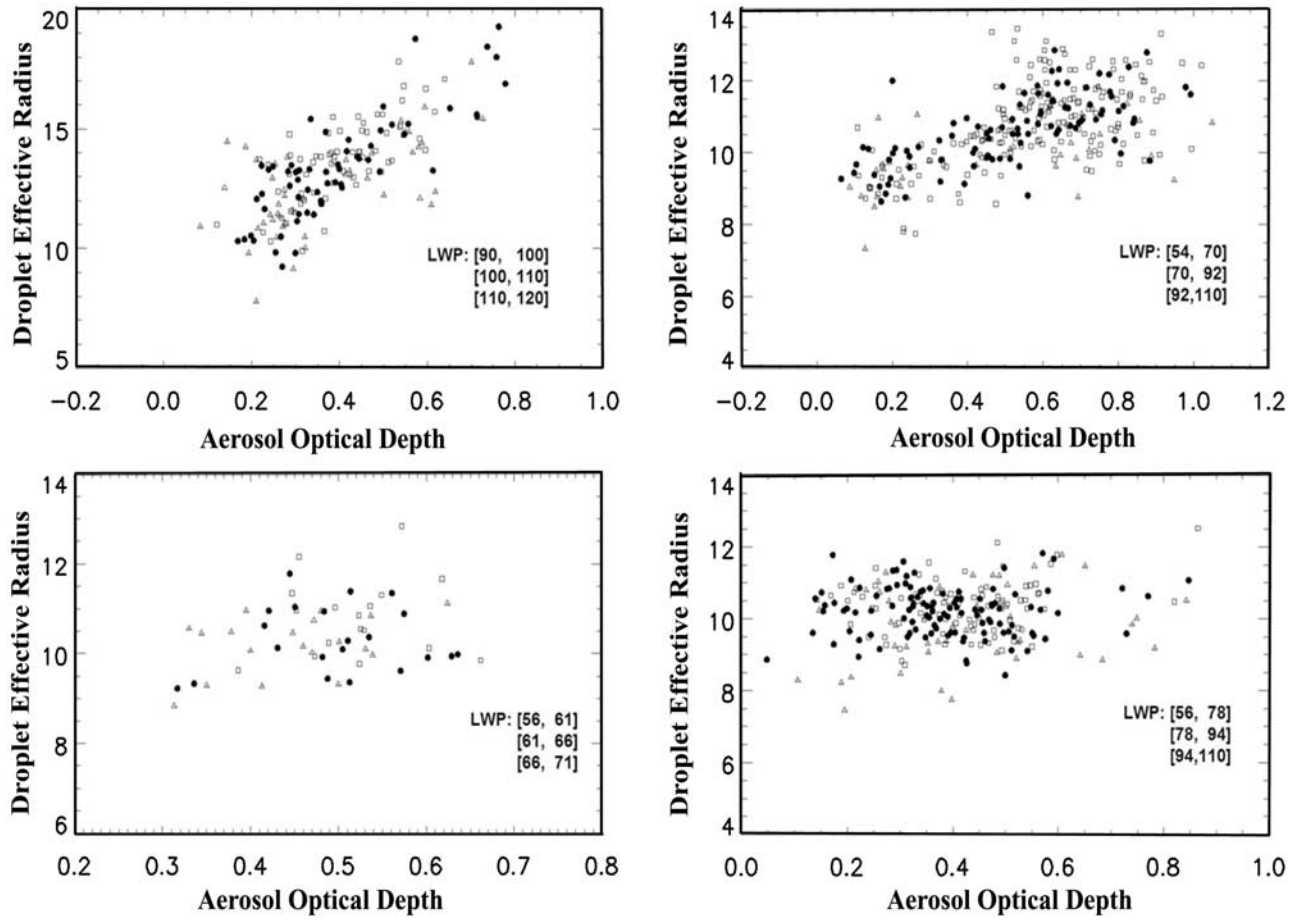

Figure 13. The AOD-DER relations by limiting the range of LWP to three narrow intervals as indicated in each panel. The intervals are so chosen based on the histogram of the frequency of occurrence in LWP distribution so that each interval contains similar number of data points.

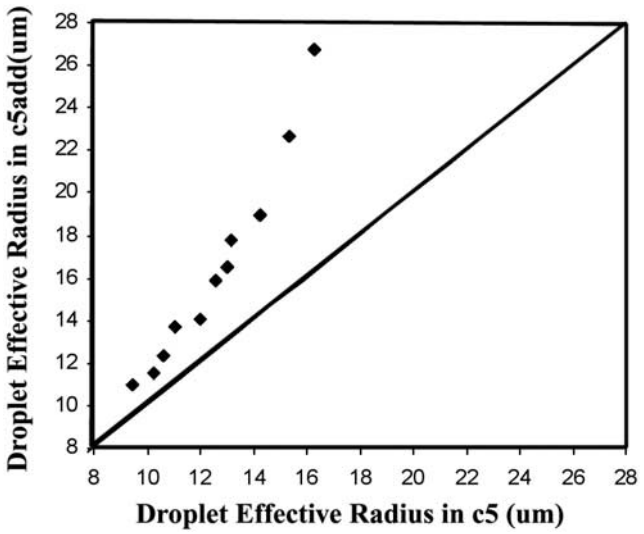

Figure 14. Comparison of DER for two simulations at different times, c5 with only small aerosol particles and c5add with giant CCNs and more aerosol particles.

exists in a warm and humid environment (with relative humidity of 87% at the surface). Simulations with a reduction of 15% in relative humidity show that the AIE efficiency is not positive anymore, supporting the correlation between AIE efficiency and water vapor amount.

[34] To verify the modeling results, we estimated the DNC from COD and DER following the method of *Han et al.* [1998]. Figure 12 shows that DNC decrease with AOD when the AIE efficiency is positive and vice versa. The slopes between AOD and DNC correlate well with the AIE efficiency and have a correlation coefficient of -0.8. The positive AIE efficiency and the negative slope between AOD and DNC suggest that the relationship between DNC and DER appears to be at odds with the Twomey's hypothesis. It is worth noting, however, that LWP increases with AOD in our case, while the Twomey's hypothesis assumes a constant LWP. The assumption is not always valid [*Twohy et al.*, 2005] and an increase of LWP with AOD has been reported [*Peng et al.*, 2002]. To constrain the variability caused by changes in LWP, we first apply strict filters to keep only high quality data (discussed in previous sections) and limit LWP variation to three narrow ranges and re-plot DER against AOD as shown in Figure 13. The AIE still shows positive relation. It should be pointed out that LWP is not an independent measurement in our analysis but retrieved from COD and DER. Direct and independent measurements of LWP are needed to verify the estimates of LWP as pointed out by *Brenguier et al.* [2003].

5.2.3. Giant CCN

[35] *O'Dowd et al.* [1999] show that giant CCNs can reduce the number of cloud droplets under polluted conditions by suppressing the supersaturation reached in a cloud based on their in situ observations and parcel model simulations. The reduced cloud droplet number concentration together with presence of giant CCNs could lead to increased droplet effective radius [*Lu and Seinfeld*, 2005]. Giant CCNs also have great potential to ignite the coalescence process in cloud development, as demonstrated by both model simulation [*Feingold et al.*, 1999] and observation [*Hindman et al.*, 1977]. To simulate the impact of giant CCN, we employ the same cloud resolving model to perform additional sensitivity studies by increasing the aerosol concentration to about 1910 cm^{-3} from controlled simulation of 1610 cm^{-3} with inclusion of giant aerosol particles at the concentration of 0.02 cm^{-3} to the bins with radii from 0.5 to 2.0 μm. The giant CCN was assumed to have the same compositions with the rest of aerosols (i.e., ammonia sulfate with SSO) in our model simulations because of the model limits. In reality, sea salt is the most likely giant CCN in this region because sea salt particles can be transported inland as giant CCNs in the summer season along the coast of the Gulf [*Verma et al.*, 2006]. A discernible increase in DER was found due to the addition of giant CCN as in Figure 14.

[36] *Dusek et al.* [2006] studied the cloud-nucleating ability by aerosol particles in terms of relative importance of chemical composition and size distribution using measurements made in Germany. It was found that the particle size distribution plays a lot more important role than chemical composition. Without in situ and coincident measurements of aerosol and CCN in our study region, it remains an open question if this is also the case for our study. In any event, the issue warrants a further investigation that requires acquisition of many in situ observations.

6. Summary

[37] Aerosol indirect forcing (AIF) is the most uncertain among all forcing factors in the climate system. Some estimates of the AIF were made based on empirical relationships between aerosol and cloud properties obtained under specific conditions, although cloud particle size is affected by numerous factors pertaining to aerosol, atmospheric environment and the dynamics. To date, the observed relationships between cloud droplet effective radius (DER) and aerosol loading which is often measured in terms of aerosol optical depth (AOD) are overwhelmingly negative with variable sensitivity. Presented in this paper are extensive analyses of the aerosol and cloud retrieved products from the Moderate Resolution Imaging Spectroradiometer (MODIS) satellite. It was revealed that the DER may increase or decrease with the AOD. While the vast majority of the regions selected around the globe exhibit negative relations between DER and AOD, a few locations show positive dependence including the Gulf coast that is scrutinized in this study. A major effort is devoted to separate real effects from artifacts.

[38] Various artifact explanations are identified and analyses were conducted to evaluate their influence on the relationship between AOD and DER. First, we employed four techniques to assess the influence of partially cloudy effect, which can increase both DER and AOD retrievals in neighboring pixels because of partially cloudy pixels. It is demonstrated that this effect is unlikely to be the cause for the correlation between AOD and DER because neither the brokenness of clouds, nor the connectivity of clouds, nor cloud fraction has a dominating effect. The cloud 3-D effect could be the most serious problem in interpreting the results obtained across a large range of scattering direction. However, little difference was found by using data from narrow strips of the MODIS images relative to the entire swath. The

third potential artifact is concerned with the aerosol swelling effect, whereby AOD increases with PW. DER may also increase with PW due to water vapor availability. While positive correlations were found for a few cases, they are too weak and variable to explain the tight correlations between AOD and DER. Both AOD and DER can also correlate highly with cloud height because of air convergence and the dependence of DER on cloud height, respectively. We reanalyze the correlation between DER and AOD for narrow intervals of cloud brightness temperature, a proxy of cloud depth, and still get positive relationships. To minimize the influence of surface condition on the AOD retrieval, similar analyses were conducted using MODIS DER and AOD data over oceans and MISR AOD data over land, noting that the MISR retrieval of AOD is least affected by surface reflection. Similar correlations between AOD and DER are found. These analyses attest that the positive correlation found between DER and AOD is likely a true physical phenomenon. This is reinforced by more compelling evidence revealed from a global survey. Negative relations were found for the majority of cases that are consistent with previous studies. Our global analysis also attests to the importance and need for taking into account factors like aerosol characteristics, circulation pattern and cloud types when studying the aerosol indirect effect (AIE).

[39] We explored potential mechanisms that can explain observed positive AIE efficiency using a 2-D version of a state-of-the-art cloud resolving model, the Goddard Cumulus Ensemble (GCE) model [*Tao et al.*, 2003] that has detailed spectral-bin microphysics. The inputs to the model were selected based on the unique atmospheric environments of the region. For aerosols, special consideration was made to slightly soluble organics (SSO) that is particularly rich over the Gulf region. To take into account the effect of SSO on aerosol activation process, the Köhler theory [*Fan et al.*, 2007] was reformulated. Using observed atmospheric sounding data, we are able to simulate cumulus clouds and the effects of several aerosol species. Positive relationships were found between cloud DER and aerosol optical depth or aerosol total concentration. The positive relationship appears to originate from a decreased number of activated cloud droplets with increasing SSO. Similar results were also obtained if giant CCNs are introduced in the model. The dependence of AIE efficiency on water vapor amount is also demonstrated in the model simulation.

[40] Despite of the many painstaking investigations by means of observation and modeling, the utter complexity of the issue and inherent limitations of satellite data prevent us from reaching a definitive conclusion regarding both the effect and its causes. However, the study does present sufficient evidence to warrant further exploration of this important phenomenon using detailed field measurements of aerosol characteristics and cloud properties.

[41] **Acknowledgments.** This study was supported by the National Science Foundation (ATMO425069), DOE DEFG0201ER63166 and the National Basic Research Program (2006CB403702). We are grateful to numerous scientists for their comments, to name a few, D. Rosenfeld, L. Remer and the late Y. Kaufman. We also wish to thank the MODIS teams and DAAC for producing and distributing the products used in the study.

References

Albrecht, B. A. (1989), Aerosols, cloud microphysics, and fractional cloudiness, *Science*, *245*, 1227–1230.

Anderson, T. H., R. J. Charlson, S. E. Schwartz, R. Knutti, O. Boucher, H. Rodhe, and J. Heintzenberg (2003), Climate forcing by aerosols-a hazy picture, *Science*, *300*, 1103.

Andreae, M. O., D. Rosenfeld, P. Artaxo, A. Costa, G. Frank, K. Longo, and M. Silva_dias (2004), Smoking rain clouds over the Amazon, *Science*, *303*, 1337–1342.

Boucher, O., and U. Lohmann (1995), The sulfate-CCN-cloud albedo effect: A sensitivity study using two general circulation models, *Tellus, Ser. B.*, *47*, 281–300.

Brenguier, J. L., H. Pawlowska, and L. Schuller (2003), Cloud microphysical and radiative properties for parameterization and satellite monitoring of the indirect effect of aerosol on climate, *J. Geophys. Res.*, *108*(D15), 8632, doi:10.1029/2002JD002682.

Broekhuizen, K., P. P. Kumar, and J. P. D. Abbatt (2004), Partially soluble organics as cloud condensation nuclei: Role of trace soluble and surface active species, *Geophys. Res. Lett.*, *31*, L01107, doi:10.1029/2003GL018203.

Dusek, U., et al. (2006), Size matters more than chemistry for cloud-nucleating ability of aerosol particles, *Science*, *312*, 1375–1377.

Facchini, M. C., M. Mircea, S. Fuzzi, and R. J. Charlson (1999), Cloud albedo enhancement by surface-active organic solutes in growing droplets, *Nature*, *401*, 257–259.

Fan, J., R. Zhang, G. Li, J. Nielsen-Gammon, and Z. Li (2005), Simulations of fine particulate matter ($PM_{2.5}$) in Houston, Texas, *J. Geophys. Res.*, *110*, D16203, doi:10.1029/2005JD005805.

Fan, J., R. Zhang, D. Collins, and G. Li (2006), Contribution of secondary condensable organics to new particle formation: A case study in Houston, Texas, *Geophys. Res. Lett.*, *33*, L15802, doi:10.1029/2006GL026295.

Fan, J., R. Zhang, G. Li, W.-K. Tao, and X. Li (2007), Simulations of cumulus clouds using a spectral microphysics cloud-resolving model, *J. Geophys. Res.*, *112*, D04201, doi:10.1029/2006JD007688.

Feingold, G., W. R. Cotton, S. M. Kreidenweis, and J. T. Davis (1999), The impact of giant cloud condensation nuclei on drizzle formation in stratocumulus: Implications for cloud radiative properties, *J. Atmos. Sci.*, *56*, 4100–4117.

Feingold, G., L. A. Remer, J. Ramaprasad, and Y. J. Kaufman (2001), Analysis of smoke impact on clouds in Brazilian biomass burning regions: An extension of Twomey's approach, *J. Geophys. Res.*, *106*, 22,907–22,922.

Feingold, G., W. L. Eberhard, D. E. Veron, and M. Previdi (2003), First measurements of the Twomey effect using ground-based remote sensors, *Geophys. Res. Lett.*, *30*(6), 1287, doi:10.1029/2002GL016633.

Gao, B. C., and Y. J. Kaufman (2003), Water vapor retrievals using Moderate Resolution Imaging Spectroradiometer (MODIS) near-infrared channels, *J. Geophys. Res.*, *108*(D13), 4389, doi:10.1029/2002JD003023.

Gao, B. C., P. Yang, W. Han, R. R. Li, and W. J. Wiscombe (2002), An algorithm using visible 1.38 channels to retrieve cirrus cloud reflectances from aircraft and satellite data, *IEEE Trans. Geosci. Remote Sens.*, *40*, 1659–1668.

Han, Q., W. B. Rossow, and A. A. Lacis (1994), Near-global survey of effective droplet radii in liquid water clouds using ISCCP data, *J. Clim.*, *7*, 465–497.

Han, Q., W. B. Rossow, J. Chou, and R. M. Welch (1998), Global variations of column droplet concentration in low-level clouds, *Geophys. Res. Lett.*, *25*, 1419–1422.

Hanel, G. (1976), The properties of atmospheric aerosol particles as function of the relative humidity at thermodynamic equilibrium with the surrounding moist air, *Adv. Geophys.*, *19*, 73–188.

Hegg, D. A., and Y. J. Kaufman (1998), Measurements of the relationship between submicron aerosol number and volume concentration, *J. Geophys. Res.*, *103*, 5671–5678.

Hindman, E. E., P. V. Hobbs, and L. F. Radke (1977), Cloud condensation nuclei from a paper mill, Part I: Measured effects on clouds, *J. Atmos. Sci.*, *16*, 745–752.

IPCC (2001), Climate Change 2001: The Scientific Basis. Contribution of Working Group I to the Third Assessment Report of the Intergovernmental Panel on Climate Change, Cambridge University Press, United Kingdom and New York, NY, USA, 881 pp.

Jeong, M.-J., Z. Li, E. Andrews, and S.-C. Tsay (2007), Effect of aerosol humidification on the column aerosol optical thickness over the Atmospheric Radiation Measurement Southern Great Plains site, *J. Geophys. Res.*, *112*, D10202, doi:10.1029/2006JD007176.

Kahn, R., B. Gaitley, J. Martonchik, D. Diner, K. Crean, and B. Holben (2005), Multiangle Imaging SpectroRadiometer (MISR) global aerosol optical depth validation based on two years of coincident AERONET observations, *J. Geophys. Res.*, *110*, D10S04, doi:10.1029/2004JD004706.

Kaufman, Y. J., and R. S. Fraser (1997), The effect of smoke particles on clouds and climate forcing, *Science*, *277*, 1636–1639.

Kaufman, Y. J., A. Seltzer, D. Ward, D. Tanre, B. Holben, P. Menzel, M. Pereira, and R. Rasmussen (1992), Biomass burning aireborne and spaceborne experiment in the Amazonas (Base-A), *J. Geophys. Res.*, *97*, 14,581–14,599.

Kaufman, Y. J., D. Tanré, L. Remer, E. F. Vermote, A. Chu, and B. N. Holben (1997), Operational remote sensing of tropospheric aerosol over the land from EOS-MODIS, *J. Geophys. Res.*, *102*(14), 17,051–17,068.

Kaufman, Y. J., P. V. Hobbs, V. Kirchoff, P. Artaxo, L. Remer, B. Holben, M. D. King, D. Ward, E. Prins, K. Longo, L. Mattos, C. Nobre, J. Spinhirne, Q. Ji, A. Thompson, J. Gleason, S. Christopher, and S. C. Tsay (1998), Smoke, Clouds, and Radiation-Brazil (SCAR-B), experiment, *J. Geophys. Res.*, *103*, 31,783–31,808.

Kaufman, Y. J. N., B. Gobron, J. L. Pinty, Widlowski, and M. M. Verstraete (2002), Relationship between surface reflectance in the visible and mid-IR used in MODIS aerosol algorithm – Theory, *Geophys. Res. Lett.*, *29*(23), 2116, doi:10.1029/2001GL014492.

Kim, B.-G., S. E. Schwartz, M. A. Miller, and Q. Min (2003), Effective radius of cloud droplets by ground-based remote sensing: Relationship to aerosol, *J. Geophys. Res.*, *108*(D23), 4740, doi:10.1029/2003JD003721.

King, M. D., Y. J. Kaufman, W. P. Menzel, and D. Tanré (1992), Remote sensing of cloud, aerosol and water vapor properties from the Moderate Resolution Imaging Spectrometer (MODIS), *IEEE Trans. Geosci. Remote Sens.*, *30*, 2–27.

Laaksonen, A., P. Korhonen, M. Kulmala, and R. J. Charlson (1998), Modification of the Köhler Equation to include soluble trace gases and slightly soluble substances, *J. Atmos. Sci.*, *55*, 853–862.

Leaitch, W. R., C. M. Banic, G. A. Isaac, M. D. Couture, P. S. K. Liu, I. Gultepe, L. Kleinman, P. H. Daum, and J. I. MacPherson (1996), Physical and chemical observations in marine stratus during the 1993 North Atlantic Regional Experiment: Factors controlling cloud droplet number concentration, *J. Geophys. Res.*, *101*, 29,123–29,135.

Liu, Y., and P. H. Daum (2002), Indirect warming effect from dispersion forcing, *Nature*, *419*, 580.

Liu, G., H. Shao, J. A. Coakley Jr., J. A. Curry, J. A. Haggerty, and M. A. Tschudi (2003), Retrieval of cloud droplet size from visible and microwave radiometric measurements during INDOEX: Implication to aerosols' indirect radioactive effect, *J. Geophys. Res.*, *108*(D1), 4006, doi:10.1029/2001JD001395.

Lohmann, U., and G. Lesins (2002), Stronger constraints on the anthropogenic indirect aerosol effect, *Science*, *298*, 1012–1015.

Lu, M., and J. H. Seinfeld (2005), Study of the aerosol indirect effect by large-eddy simulation of marine stratocumulus, *J. Atmos. Sci.*, *62*, 3909–3932.

Martins, J. V., D. Tanre, L. Remer, Y. J. Kaufman, S. Mattoo, and R. Levy (2002), MODIS cloud screening for remote sensing of aerosols over oceans using spatial variability, *Geophys. Res. Lett.*, *29*(12), 8009, doi:10.1029/2001GL013252.

Miller, M. A., B. A. Albrecht, and E. E. Clothiaux (1998), Diurnal cloud and thermodynamic variations in the stratocumulus transition regime: A case study using in situ and remote sensors, *J. Atmos. Sci.*, *55*, 2294–2310.

Nakajima, T., and A. Higurashi (1998), A use of two-channel radiances for an aerosol characterization from space, *Geophys. Res. Lett.*, *25*, 3815–3818.

Nakajima, T., and M. D. King (1990), Determination of theoretical thickness and effective particle radius of clouds from reflected solar radiation measurements, Part I: Theory, *J. Atmos.*, *47*, 1878–1893.

Nakajima, T., A. Higurashi, K. Kawamoto, and J. E. Penner (2001), A possible correlation between satellite-derived cloud and aerosol microphysical parameters, *Geophys. Res. Lett.*, *28*, 1171–1174.

O'Dowd, C. D., J. Lowe, M. H. Smith, and A. D. Kaye (1999), The relative importance of sea-salt and nss-sulphate aerosol to the marine CCN population: An improved multi-component aerosol-droplet parameterisation, *Q. J. R. Meteorol. Soc.*, *125*, 1295–1313.

Peng, Y., U. Lohmann, R. Leaitch, C. Banie, and M. Couture (2002), The cloud albedo-cloud droplet effective radius relationship for clean and polluted clouds from RACE and FIRE, ACE, *J. Geophys. Res.*, *107*(D11), 4106, doi:10.1029/2000JD000281.

Penner, J. E., X. Dong, and Y. Chen (2004), Observational evidence of a change in radiative forcing due to the indirect aerosol effect, *Nature*, *427*, 231–234.

Platnick, S., and S. Twomey (1994), Determining the susceptibility of cloud albedo to changes in droplet concentration with the advanced very high resolution radiometer, *J. Appl. Meteorol.*, *33*, 334–347.

Platnick, S., M. D. King, S. A. Ackerman, W. P. Menzel, B. A. Baum, J. C. Riedi, and R. A. Frey (2003), The MODIS cloud products: Algorithms and examples from Terra, *IEEE Trans. Geosci. Remote Sens.*, *41*, 459–473.

Ramanathan, V., et al. (2001), Indian Ocean Experiment: An integrated analysis of the climate forcing and effects of the great Indo-Asian haze, *J. Geophys. Res.*, *106*, 28,371–28,398.

Remer, L. A., et al. (2005), The MODIS aerosol algorithm, products and validation, *J. Atmos. Sci.*, *l 62*, 947–973, Special Section.

Rosenfeld, D., and G. Feingold (2003), Explanation of discrepancies among satellite observation of aerosol indirect effects, *Geophys. Res. Lett.*, *30*(14), 1776, doi:10.1029/2003GL017684.

Rosenfeld, D., and I. M. Lensky (1998), Satellite based insights into precipitation formation processes in continental and maritime convective clouds, *Bull. Am. Meteorol. Soc.*, *79*, 2457–2476.

Rotstayn, L. D., and Y. G. Liu (2003), Sensitivity of the first aerosol indirect effect to an increase of cloud droplet spectral dispersion with droplet number concentration, *Clim. J.*, *16*, 3476–3481.

Russell, M., D. T. Allen, D. R. Collins, and M. P. Fraser (2004), Daily, seasonal and spatial trends in $PM_{2.5}$ mass and composition in southeast Texas, *Aerosol Sci. Technol.*, *38*, 14–26.

Sekiguchi, M., T. Nakajima, K. Suzuki, K. Kawamoto, A. Higurashi, D. Rosenfeld, I. Sano, and S. Mukai (2003), A study of the direct and indirect effects of aerosols using global satellite data sets of aerosol and cloud parameters, *J. Geophys. Res.*, *108*(D22), 4699, doi: 10.1029/2002JD003359.

Shantz, N. C., W. R. Leaitch, and P. F. Caffrey (2003), Effect of organics of low solubility on the growth rate of cloud droplets, *J. Geophys. Res.*, *108*(D5), 4168, doi:10.1029/2002JD002540.

Sheridan, P. J., D. J. Delene, and J. A. Ogren (2001), Four years of continuous surface aerosol measurements from the Department of Energy's Atmospheric Radiation Measurement Program Southern Great Plains Cloud and Radiation Testbed site, *J. Geophys. Res.*, *106*, 20,735–20,747.

Strorelvmo, T., J. E. Kristjansson, G. Myhre, M. Johnsrud, and F. Stordal (2006), Combined observational and modeling based study of the aerosol indirect effect, *Atmos. Chem. Phys.*, *6*, 3583–3601.

Tao, W.-K., et al. (2003), Microphysics, radiation and surface processes in the Goddard Cumulus Ensemble (GCE) model, *Meteorol. Atmos. Phys.*, *82*, 97–137.

Twohy, C. H., M. D. Petters, J. R. Snider, B. Stevens, W. Tahnk, M. Wetzel, L. Russell, and F. Burnet (2005), Evaluation of the aerosol indirect effect in marine stratocumulus clouds: Droplet number, size, liquid water path, and radiative impact, *J. Geophys. Res.*, *110*, D08203, doi:10.1029/2004JD005116.

Twomey, S. A. (1977), The influence of pollution on the shortwave albedo of clouds, *J. Atmos.*, *34*, 1149–1152.

Vant-Hull, B., A. Marshak, L. Remer, and Z. Li (2006), The effects of scattering angle and cumulus cloud geometry on satellite retrievals of cloud drop effective radius, *IEEE TGRS.*, accepted.

Vant-Hull, B., A. Marshak, L. Remer, and Z. Li (2007), The effects of scattering angle and cumulus cloud geometry on satellite retrievals of cloud drop effective radius, *IEEE Geosci. Rem. Sens. Lett.*, *45*, 1039–1045.

Verma, S., O. Boucher, C. Venkataraman, M. S. Reddy, D. Müller, P. Chazette, and B. Crouzille (2006), Aerosol lofting from sea breeze during the Indian Ocean Experiment, *J. Geophys. Res.*, *111*, D07208, doi:10.1029/2005JD005953.

Wen, G., A. Marshak, and R. F. Cahalan (2006), Impact of 3D clouds on clear sky reflectance and aerosol retrieval in a biomass burning region of Brazil, *IEEE Trans. Geosci. Remote Sens. Lett.*, *3*, 169–172.

Wetzel, M. A., and L. L. Stowe (1999), Satellite-observed patterns in stratus cloud microphysics, aerosol optical thickness and shortwave radiative forcing, *J. Geophys. Res.*, *104*, 31,286–31,299.

Young, K. C. (1993), Microphysics processes in clouds, Oxford University Press, Inc., New York, New York.

Zhang, R., I. Suh, J. Zhao, D. Zhang, E. C. Fortner, X. Tie, L. T. Molina, and M. J. Molina (2004), Atmospheric new particle formation enhanced by organic acids, *Science*, *304*, 1487–1490.

J. Fan and R. Zhang, Dept. of Atmospheric Sciences, University of Texas A&M, College Station, TX 77843, USA.

Z. Li and T. Yuan, Dept. of Atmospheric and Oceanic Science and ESSIC, University of Maryland, College Park, MD 20742, USA. (zli@atmos.umd.edu)